Eng. Sci., 2021, **16**, 308–318

Engineered Science

DOI: https://dx.doi.org/10.30919/es8d571

Ultra-Massive Multiple Input Multiple Output Technologies for 6G Wireless Networks

Ravilla Dilli,[1,*] Ravi Chandra M L[2,#] and Deepthi Jordhana[3,#]

Abstract

The increasing global demand for ultra-high spectral efficiencies, data rates, speeds, and bandwidths in next-generation wireless networks motivate the exploration of peak capabilities of ultra-massive multiple input multiple output (mMIMO) wireless access technology at THz bands (0.1 THz – 10 THz). The smaller wavelengths (in the order of microns) of these frequencies give an advantage of making possible high gain antennas with smaller physical dimensions and allowing massive spatial multiplexing. This paper presents the design of an ultra-mMIMO hybrid beamforming system for multi users and its feasibility to function at THz frequency bands. The functionality of the proposed system is verified rigorously using higher order modulation schemes to have higher spectral efficiencies using performance metrics that includes error vector magnitude, symbol constellations, and antenna array radiation beams. The performance results suggest to use a particular mMIMO antenna configuration based on the number of independent data streams/user and strongly suggested to use maximum number of data streams/user in order to achieve higher throughputs that satisfy the needs of 6G wireless systems. Also the performance of proposed system at 0.14 THz is compared with mmWave hybrid beamforming systems that operate at 28 GHz and 73 GHz bands.

Keywords: 6G wireless communication; Hybrid beamforming; Massive MIMO; Multi-input-multi-output; Spatial multiplexing; THz band.

Received: 26 July 2021; Accepted: 11 November 2021.

Article type: Research article.

1. Introduction

The 5G wireless technology will be inadequate in the near future due to the explosive growth of device-to-device (D2D) networks like IoT, IIoT, IoS, and IoE. The 6G wireless communication systems are aimed at supporting the communication needs of 2030 s. Therefore, 6G wireless technology which uses terahertz (0.1 THz – 10 THz) EM spectrum frequencies that supports 10 GHz – 100 GHz bandwidths, and data rates of terabits/sec are essential.[1-3] The 6G wireless system architecture is an integrated system of different radio access technologies with ultra-massive scales and dynamic network resources to achieve diverse performance improvements. The radio network architecture of 6G cellular systems should make use of features like cognitive radio, carrier aggregation, THz bands, ultra- massive multiple input multiple output (mMIMO), and femtocell-based heterogeneous networks to provide maximum capacity. The key differences in performance indicators of 5G and 6G communication systems are mentioned in Table 1. The main aim of this article is to propose and design a hybrid beamforming system for 6G wireless networks that consist of ultra-mMIMO antenna array configurations of size that varies from 64 to 256 at BS and 4 to 16 at MS of multiple users that operates in the 0.14 THz frequency band. The performance measurements are noted at 0.14 THz frequency band and feasibility of the proposed system is verified using higher order quadrature amplitude modulation (QAM) schemes, also the results are compared with mmWave hybrid beamforming systems that operate in the 28 GHz and 73 GHz bands.

[1] *Associate Professor, Department of Electronics and Communication Engineering, Manipal Institute of Technology, Manipal Academy of Higher Education, Manipal, Udupi District, Karnataka, India.*

[2] *Professor and Head, Department of Electronics and Communication Engineering, Srinivasa Ramanujan Institute of Technology, Ananthapuramu, Andhra Pradesh, India.*

[3] *Professor, Department of Electronics and Communication Engineering, Srinivasa Ramanujan Institute of Technology, Ananthapuramu, Andhra Pradesh, India.*

**E-mail:* dilli.ravilla@manipal.edu (Ravilla Dilli)

[#] *These authors contributed to this work equally.*

© Engineered Science Publisher LLC 2021

Table 1. Key Performance Indicators of 5G and 6G Communication Systems.

Key performance Indicator	5G	6G
Technologies	mMIMO, mmWave bands, network densification, polar codes, LDPC codes, cloud/fog/edge computing	Cell-free mMIMO, RIS, AI, Quantum communications & computing
Multiplexing/Multiple Access Techniques	OFDM, Adaptive Time-Frequency Multiplexing, GFDM, FBMC	Spatial multiplexing, OMA, NOMA, OAM multiplexing
End-to-End Latency	1 msec to 10 msec	0.1 msec
Data rates	1 Gbps to 30 Gbps	100 Gbps to 1Tbps
Reliability (Packet Error Rate)	$1\text{-}10^{-5}$	$1\text{-}10^{-9}$
Mobility	500 kmph	1000 kmph
Energy efficiency	--	1 Tb/J
Delay Jitter	--	10 msec
Peak data rates	20 Gbps	1 Tbps
Experienced data rates	0.1Gbps	1 Tbps
Peak spectral efficiency	30 bits/sec/Hz	100 bits/sec/Hz
Experienced spectral efficiency	0.3 bits/sec/Hz	3 bits/sec/Hz
Maximum channel bandwidth	1 GHz	100 GHz
Connection density	10^2 Devices/100m^2	10^3 Devices/100m^2
Processing Delay	100 nsec	10 nsec
Frequency bands	Sub-GHz, mmWave	THz Bands, Non-RF (VLC, optical range), block-chain based spectrum sharing
Use cases	eMBB, URLLC, mMTC	MBRLLC, mURLLC, human-centric services
Device types	Smart phones, sensors, drones	Smart implants, CRAS, sensors and DLT, XR and BCI
Traffic capacity	10 Mbps/m^2	10 Gbps/m^3
Localization precision	10cm in 2-dimensional	1cm in 3-dimensional
Reliability	99.9%	99.999%
Receiver sensitivity	About -120dBm	Less than -130dBm

1.1 Enabling technologies and challenges for 6G

Current 5G wireless networks have insufficient computing capabilities, high interference because of massive interconnection, absence of ubiquitous connectivity and they are unable to meet the high-speed applications like holographic communication that needs 1Tbps for seamless communication. To meet the near future demands and facilitate extremely high bandwidth, low latency, high data rates, high reliability, and low-energy consumption applications of wireless networks, 6G is proposed. 6G applications include holographic communication, industry 4.0, remote operated driving, tactile internet, *etc.*

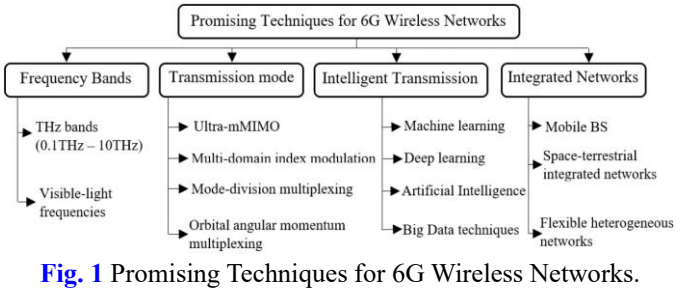

Fig. 1 Promising Techniques for 6G Wireless Networks.

AI was already introduced in 5G, we envision that AI techniques like machine learning, deep learning plays a major role in achieving smart, intelligent 6G networks. As RIS enables enhanced, ubiquitous connectivity, and these have advantages over relay systems. RISs are deployed on buildings, doors, windows, and the reflected signals from RIS help in serving areas where LoS is tricky.[4] Technologies like RIS, UAV, pervasive AI, Cell-free mMIMO, THz bands, quantum communication, ambient backscatter communication (for wireless charging), block-chain, and optical wireless technology as shown in Fig. 1 enhances the computing efficiencies, and security of 6G wireless networks.

This paper is organized as follows: Section 1 provides insight into design challenges, key enabling technologies, role of AI, and security aspects in 6G wireless networks. Section 2 explores the signal characteristics, wave propagation at THz frequency bands. Section 3 describes channel modelling and measurements at THz bands. Section 4 explores the possibility of using ultra-massive MIMO hybrid beamforming techniques for improved front-end performance at frequencies above 100 GHz. Section 5 discusses the results of ultra-massive MIMO hybrid beamforming system at 140 GHz and compare them with the system performance at 28 GHz, and 73 GHz mmWave frequencies.[5] Section 6 gives overall observations, conclusions, and possible future directions of the research that can be carried out towards the use of THz frequency bands.

© Engineered Science Publisher LLC 2021

2. Signal characteristics at THz frequencies

The radio signal propagation undergoes through three main propagation mechanisms called reflection, diffraction, and scattering in multipath channel.[6] At THz carrier frequencies, signal transmissions are highly directive (less angular divergence) and diffraction effects are minimum. Adaptation of mMIMO, hybrid beamforming or beam steering techniques overcomes the shadowing effects at mmWave frequencies.[7] Scattering is an important propagation mechanism to consider in channel modelling at THz frequencies for 6G wireless systems. The surface scattering at THz frequencies exhibit both diffuse and strong specular reflections. "Directive scattering" and "radar cross section" scattering models support development of ray tracing tool design, imaging, and localization for 6G wireless systems.[8] Characterization of surface scatterers (for both diffused and specular components) at 60 GHz leads to small-scale fading due to rough surface scatterers. The diffused scattering depends on distance from the surface, angle of incidence, and material roughness.[9] The multipath delay spread and path losses of a radio channel are characterized at frequency range 126 GHz – 156 GHz.[10] The wavelengths of THz frequencies approach the dimensions of dust, snow particles or rain, and effects of Mie scattering becomes more significant contribution to link budget. The rain effects do not contribute to additional attenuation losses at THz frequencies (0.1 THz–0.5 THz).[11] Atmospheric gases like hydrogen, oxygen, and carbon-di-oxide *etc.* cause significant attenuation at THz bands (183 GHz, 325 GHz, 380 GHz, 450 GHz, 550 GHz and 760 GHz) and these frequency bands can be used for secure ultra-short range communications.[12-13]

3. Channel modelling and measurements at THz bands

Channel properties define the performance limits in 6G wireless communication systems. Therefore, it is very important to explore different 6G channel models, measurement techniques, and develop statistical channel impulse response models at THz frequencies both in space and time.[14-16] The requirement of high data rates and bandwidths for smart rail mobility motivates to explore high gain mMIMO, advanced handover designs, and dynamic beamforming techniques at mmWave and THz bands.[17] The communication between passengers and rails as well as intra-wagon scenarios are characterized using ultra-wideband channel sounding and ray tracing at 60 GHz and 300 GHz frequency bands with 8 GHz of bandwidth.[18] The measured propagation losses of a communication link at 350 GHz frequency estimates the data rates of 1 Gbps at 8.5m and 100 Gbps for 1m distances.[19] Channel models and propagation measurements are presented at D-band (110 GHz-170 GHz) frequencies. Channel sounder system is designed for 140 GHz and signal attenuation measurements are investigated for indoor models.[20-21] The large-scale path loss and multipath time dispersion measurements for ultra-dense indoor wireless networks at mmWave bands show that multipath RMS delay spread can be minimized using more directive antennas.[22] Certain mmWave and THz frequency bands exhibit less path loss (< 10 dB/Km) in addition to free-space path loss values. Therefore, these frequencies can be used for 6G cellular and mobile applications (long-range communications).[23] THz frequencies exhibit a very high signal attenuation or path loss, however, we can overcome this using ultra-mMIMO antenna arrays which compensate increased path loss and provides highly reliable links.[24] A careful neighbor discovery process in mMIMO systems is essential to have higher throughputs and lower interference.[25] Indoor and outdoor channel measurements at 100 GHz, 200 GHz, 300 GHz, and 400 GHz are carried out for a link data rate of 1 Gbps. The multi-path channel measurements proved the feasibility of using THz radio links for data transmissions in a highly fading channel environments.[26] The radiation at THz (0.1 THz – 10 THz) bands penetrates through materials (indoor office) with minimum penetration losses and loss increases for higher end of THz band.[27]

4. Ultra-massive MIMO and hybrid beamforming techniques for 6G

mMIMO and ultra-mMIMO are the key enabling technologies in 5G and 6G networks respectively with efficient beam steering capabilities. The important open research challenges in mMIMO system design are channel estimation, pilot contamination, user scheduling, precoding, signal detection, and energy efficiency.[28] The mMIMO and ultra-mMIMO beamforming systems offer huge bandwidths with very high data rates in 5G and 6G cellular mobile systems. They provide maximum antenna array gains by overcoming the high path loss, atmospheric absorption, and rapid channel variations. These designs demand precise alignment of BS and UE beams that increases latency in link establishment, implications of control layer procedures like beam tracking, and handover.[29] The characterization of mMIMO channel can be represented as shown in Equation 1.

$$\mathbf{y} = \mathbf{H}\ \mathbf{X} + \mathbf{n} \tag{1}$$

$$\text{The channel matrix, } \mathbf{H} = \begin{bmatrix} h_{11} & h_{12} & \dots & h_{1Mt} \\ h_{21} & h_{22} & \dots & h_{2Mt} \\ \dots & \dots & \dots & h_{3Mt} \\ h_{Mr1} & h_{Mr2} & \dots & h_{MrMt} \end{bmatrix}$$

where h_{ij} is a complex gaussian random variable to model fading gain between j^{th} Rx antenna and i^{th} Tx antenna. For any given subcarrier 'k', the vector observation is given in Equation 2.

$$\mathbf{z}_k = \mathbf{H}_k\mathbf{X}_k + \mathbf{n}_k \tag{2}$$

where $\mathbf{y} \rightarrow$ Rx column vector of size $M_r \times 1$, $\mathbf{H} \rightarrow$ channel matrix of size $M_r \times M_t$, $\mathbf{X} \rightarrow$ Tx column vector of size $M_t \times 1$, $\mathbf{n} \rightarrow$ AWGN noise column vector of size $M_r \times 1$, and $\mathbf{z}_k \rightarrow$ observation vector of size $M_r \times 1$.

In a MIMO system, transmitting one symbol over all M_t antennas leads to high diversity but with low rate. In a mMIMO system with beamforming as shown in Fig. 2 gives

 © Engineered Science Publisher LLC 2021

both diversity gain as well as higher data rates. The received symbols in such systems can be derived as given in Equation 3.

$$y = \mathbf{U}^H\mathbf{H}\mathbf{V}x + n \quad (3)$$

where x, y, n are scalars and select **U** and **V** along largest singular value.

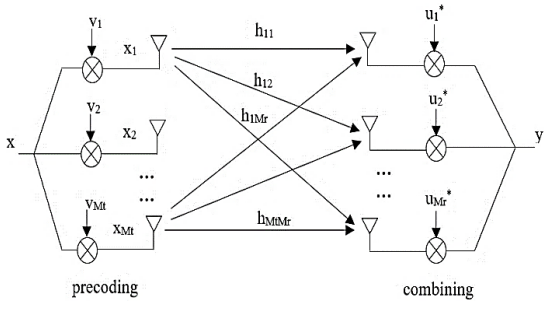

Fig. 2 mMIMO Channel with Beamforming.

The narrowband MIMO channel can be represented using Equation 4 as,

$$\mathbf{y} = \mathbf{H}\ \mathbf{x} + \mathbf{n} \quad (4)$$

where $E\{\mathbf{x}\mathbf{x}^H\} = \mathbf{R}_x\ \mathbf{R}_x \rightarrow$ input covariance matrix and $\mathbf{R}_x{}^T = \rho$ and $E\{\mathbf{n}\mathbf{n}^H\} = \mathbf{I}_{Mr}$ where **n** is zero mean gaussian noise.

Channel capacity for fixed channel,

$$C = \max\ \{B \log_2 \det\ [\mathbf{I}_{Mr} + \mathbf{H}\ \mathbf{R}_x\ \mathbf{H}^H]\} \quad (5)$$

for all $\mathbf{R}_x = \mathbf{R}_x{}^T = \rho$, the channel matrix, H can be represented as $\mathbf{H} = \mathbf{U}\mathbf{\Sigma}\mathbf{V}^H$ with $\Sigma = \text{diag}\ (\sigma_1{}^2, \sigma_2{}^2, \ldots\ \sigma_{RH}{}^2, 0, \ldots\ 0)$: The Equation 5 maximizes the overall possible covariance matrices that satisfy the total energy constraint. If the channel is unknown at the Tx (no CSIT), then the total energy spreads among all M_t Tx antennas, therefore $\mathbf{R}_x = [\rho/M_t]\ \mathbf{I}_{Mt}$ and the channel capacity is given in Equation 6.

Channel capacity,

$$C = B\ \sum_{i=1}^{RH}\ \log_2(1 + (\rho\ \sigma_i{}^2)/M_t) \quad (6)$$

On the other hand, if CSIT is available, we can do more sophisticated detection using SVD and exploit power allocation. The corresponding channel capacity is given in Equation 7.

Channel capacity,

$$C = \sum_{i=1}^{RH}\ B\log_2(1 + (\rho_i\ \sigma_i{}^2)) \text{ for all } \rho_i:\ \sum_{i=1}\ \rho_i \le \rho \quad (7)$$

In MU-mMIMO systems, users are always orthogonal and favorable propagation conditions in LOS relies on geometry of the array and far field conditions. If 'M' antenna elements spaced at $d = \lambda/2$ and the incoming signal makes an angle 'θ', then the path difference $\delta = d \sin(\theta)$. Therefore, the received passband signals are given as follows: $r_0(t) = \text{Re}\{As(t - \tau) \exp(j2\pi f_c(t - \tau))\} = \text{Re}\{gs(t) \exp(j2\pi f_c t)\}$ $r_1(t) = \text{Re}\{gs(t - \delta/c) \exp(j2\pi f_c(t - \delta/c))\} = \text{Re}\{gs(t) \exp(j2\pi f_c t)) \exp(-j2\pi f_c \delta/c)\}$ and the corresponding received baseband signals are given in Equation 8.

$$y_m(t) = gs(t)\exp(-j2\pi\delta m/\lambda),\ m = 0, M-1 \text{ and } \mathbf{y} = \mathbf{hs} + \mathbf{n} \quad (8)$$

The channel with gk being a complex number, the same for all antenna elements and given as:

$$h_k = g_k[1\ \exp^{-j2\pi d\sin(\theta k)/\lambda}\ \exp^{-j4\pi d\sin(\theta k)\ \lambda}\ \exp^{-j2(M-1)\pi d\sin(\theta k)/\lambda}]\ \theta_l$$
$$\neq \theta_k \rightarrow h^H{}_k\ h_l \approx 0$$

This allows beamforming in specific directions ($d = \lambda/2$).

5. Results and discussions

3 GPP recommends the 28 GHz, 73 GHz, and 140 GHz frequency bands for future MU-ultra-mMIMO wireless communication systems.[30-31] Therefore, system performance is verified at these frequencies for a maximum of 256 × 16 MIMO order with 4, 8 users using the simulation parameters as mentioned in Table 2. All the simulations are carried out using MATLAB tool. At the BS, rectangular antennas array of size 256 (64 rows and 4 columns) is connected to 4 - RF chains, At MS, 16 antenna elements (4 rows and 4 columns) connected to 4 - RF chains. With this design, every element of an antenna is connected to 4-phase shifters and radiation patterns of antenna arrays becomes isotropic with linear or rectangular geometry. In order to have peak spectral efficiencies, independent channels are assigned for each user and independent data streams are transmitted through each RF chain that leads to maximum of four data streams per user. The channel between UEs and BS is modeled as well as validated through "MIMO scattering-spatial channel" model. This model assumes the randomly placed scatters and presence of UE at various T-R spatial locations. The UEs of each user is modeled by compensating thermal noise and path loss. A single common channel is used for both non-LOS and LOS scenarios to model the path loss, data transmissions as well as for channel sounding. The periodic updates of channel matrix at regular intervals are essential to mimic the channel variations.

Table 2. System specifications for a MU-ultra-mMIMO system.

System Specification	Values
Number of transmitting antennas at BS	64, 128, 256
Number of antennas/user at UE	[16 4 12 4 8 4 12 4], [16 4 8 4]
Antenna array configuration	URA, ULA
Spacing between antenna elements	0.5λ
Bits/subcarrier	4, 6, 8
OFDM data symbols	10, 12, 14
Users	4, 8
Independent data streams/user	[4 1 2 1], [4 1 3 1 2 1 3 1]
UE position	Elevation Angle: [−90° 90°] Azimuthal Angle: [−180° 180°]
BS position	(0, 0)
Range at UE (maximum value)	1km
Carrier frequency	28 GHz, 73 GHz, 140 GHz
QAM order	4, 6, and 8
Channel sampling rate	100 Mbps
Channel type	Scattering, MIMO

© Engineered Science Publisher LLC 2021

Table 3. RMS EVM values in an ultra-mMIMO system for different QAM schemes at 140 GHz frequencies with 4 users.

Modulation Scheme	BS Antenna Elements	Users at 140 GHz			
		1	2	3	4
256-QAM	256	0.81258	0.86757	0.50247	0.72724
	128	0.33035	1.0522	0.563	1.1686
	64	0.13909	1.8912	0.74997	2.2471
64-QAM	256	0.84058	1.0879	0.46846	0.73867
	128	0.32361	1.1148	0.614	1.1582
	64	0.13746	1.8514	0.7483	2.2165
16-QAM	256	0.80878	0.85585	0.45633	0.73577
	128	0.32897	1.0915	0.55477	1.1415
	64	0.13855	1.9694	0.75611	2.3147
Independent data streams/user		4	1	2	1

From Table 3, it is very clear that the RMS EVM values are minimum when the number of data streams/user are high, however, the error values are increasing for users with higher data streams even when size of mMIMO system increases. When the number of data streams/user are minimum (one data stream/user, two data stream/user), the error values are higher at lower configurations of mMIMO size, however, the RMS EVM values are reducing at higher mMIMO size configurations. From the above simulation results, we can conclude that 256 × 8, 128 × 16, and 64 × 16 mMIMO configurations are optimum for 4-user mMIMO hybrid beamforming systems when the number of data streams/user are two, four and four respectively.

From Table 4, the optimum values of EVM are achieved for 256 × 16 mMIMO antenna configurations where users maintain 4 independent data streams/user, and error values are highest for 64 × 4 mMIMO configuration with one independent data stream/user. For a given BS antenna array and modulation scheme, it is clear that RMS EVM values are decreasing when the users maintain higher data streams. For a given modulation order, increasing size of BS antenna array benefits with lower RMS EVM values. However, there are very few cases where there is a little increase in RMS EVM values for BS antenna array size of 256. When the user's data is split into multiple independent parallel streams, then it needs lower active antenna elements to transmit these signals. Therefore, it gives a trade-off between data streams/user and T-R antenna array size.

5.1 Performance of MU-Ultra-mMIMO systems for 4 users

Figs. 3, 4a and 4b present the performance in terms of RMS EVM values in an ultra-MU-mMIMO system for 4 users at 140 GHz and compared with performance at 28 GHz, 73 GHz.[30] Users 1, 2, 3, and 4 transmit their data using four, one, two and one independent data streams, respectively. From Fig. 3, 4a, and 4b, it is observed that RMS EVM values are minimum for users 1 and 3 as they maintain more number of data streams for transmission. Interestingly, for user 4, the error values are minimum at 140 GHz as compared to the 28 GHz and 73 GHz frequencies. This justifies the use of THz frequencies and higher order modulation schemes to achieve higher bandwidths, data rates, and spectral efficiencies. For user 3 that maintains two independent data streams, the error values are minimum at 73 GHz and it motivates us to study the performance of MU-mMIMO hybrid beamforming at these frequencies. For user 1 which has highest number of data streams, the error values are slightly increasing at 140 GHz compared to the 73 GHz and 28 GHz frequency bands, however the errors are within the acceptable limits. Also for a given order of QAM modulation scheme and carrier that are considered in this paper, the error values are slightly increasing even at higher order mMIMO antenna array configurations for the users who maintain large number of data streams and it needs more explorations to minimize the errors in spite that they are within limits.

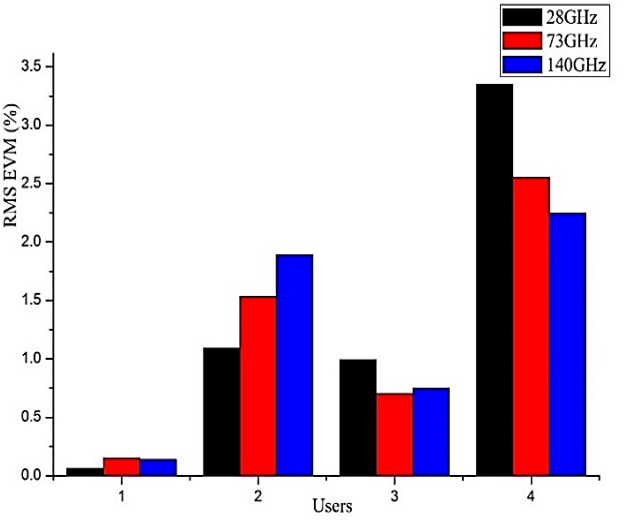

Fig. 3 Values of error vectors with 256-QAM modulation scheme using 64 BS antennas.

The 3D-signal radiation patterns in ultra-MU-mMIMO hybrid beamforming systems with multiple BS antennas array sizes for four users and eight users are shown in Figs. 5a - 5d, and Figs. 8a - 8c respectively. The stronger lobes indicate distinct data streams of users and these lobes show the spread

 © Engineered Science Publisher LLC 2021

achieved by hybrid beamforming. The observation is that the radiation beams are becoming more focused for increasing antennas array size at BS and UE which enhances the received signal reliability and there by throughput.

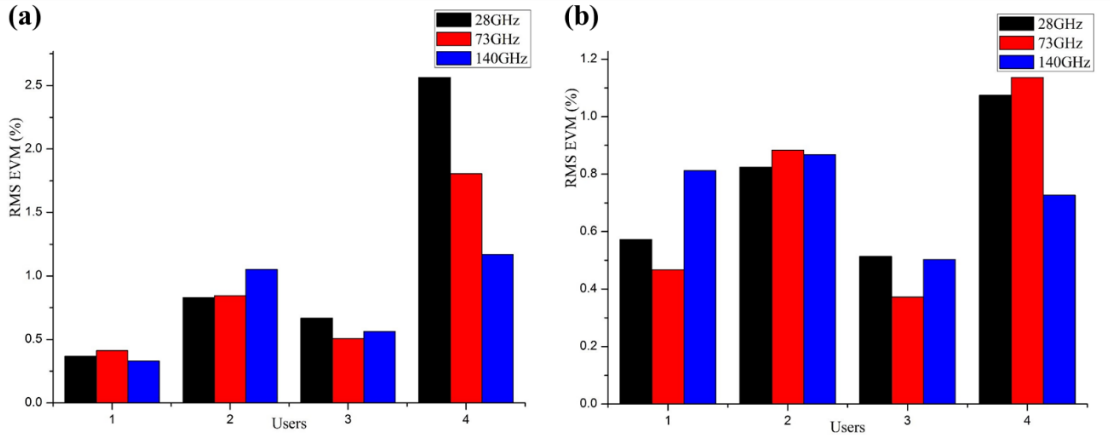

(a) 128 BS antennas (b) 256 BS antennas

Fig. 4 Values of error vectors with 256-QAM modulation scheme using different number of BS antennas.

Table 4. RMS EVM values in an ultra-mMIMO system for different QAM schemes at 140 GHz frequencies with 8 users.

Modulation Scheme	BS Antenna Elements	Users at 140 GHz							
		1	2	3	4	5	6	7	8
256-QAM	256	0.10643	9.63	0.84648	5.3012	1.7391	6.0378	1.7481	4.7462
	128	0.1249	1.0522	0.42981	5.0051	0.74358	8.8211	1.3856	5.4127
	64	0.24345	50.064	1.7185	5.8015	0.42917	16.5441	1.9911	34.3318
64-QAM	256	0.1079	15.3801	0.87072	6.3431	1.7651	9.1091	1.7298	5.1259
	128	0.12292	17.5615	0.49705	5.6778	0.73831	13.5069	1.3792	6.5138
	64	0.244	54.8285	1.7054	7.1033	0.42623	21.6397	1.992	38.67
16-QAM	256	0.10546	24.5707	0.84912	6.3027	1.7625	10.1468	1.7413	5.4381
	128	0.12308	29.4725	0.48917	5.7685	0.74072	20.579	1.3852	6.6699
	64	0.23899	0.23899	1.7292	7.2365	0.42512	30.5615	1.9993	47.1606
Independent data streams/user		4	1	3	1	2	1	3	1

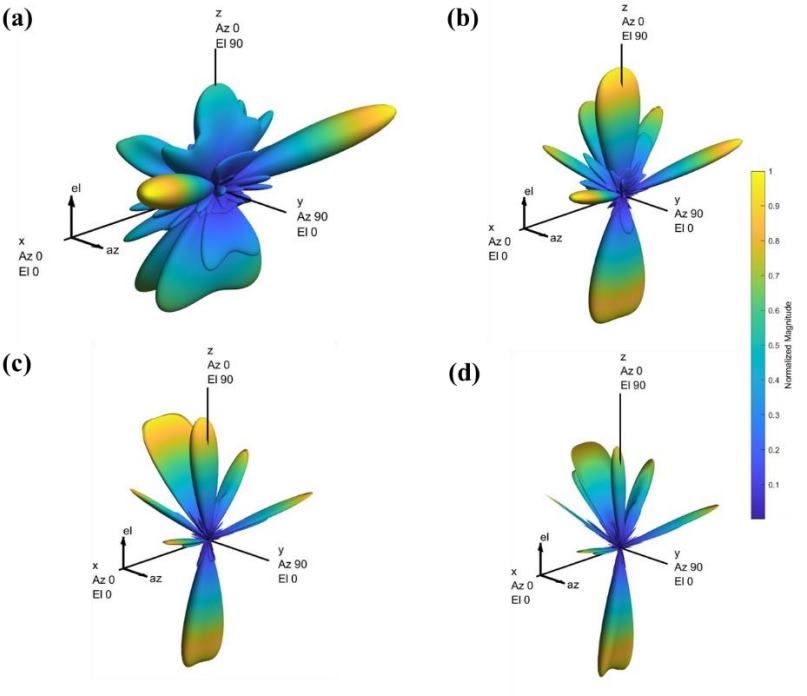

Fig. 5 Signal 3D-radiation pattern in MU-mMIMO hybrid beamforming system using 256-QAM scheme with different number of BS antennas for 4 users at 140 GHz.

© Engineered Science Publisher LLC 2021

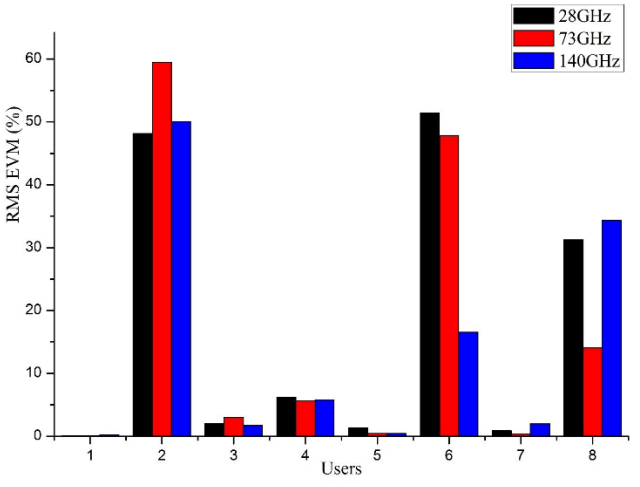

Fig. 6 Values of RMS error vectors in a MU-mMIMO hybrid beamforming system using 256-QAM modulation scheme with 64 BS antennas.

5.2 Performance of MU-Ultra-mMIMO systems for 8 users

Figs. 6, 7a and 7b present the performance in terms of RMS EVM values in an ultra-MU-mMIMO systems for eight users at 140 GHz and compared with the performance at 28 GHz, and 73 GHz.[30] Users 1, 2, 3, 4, 5, 6, 7, and 8 transmit their data using four, one, three, one, two, one, three, and one independent data streams, respectively. From Figs. 6, 7a and 7b, it is observed that RMS EVM values are minimum for users 1, 3, 5, and 7 as they maintain a higher number of data streams for transmission. Interestingly, for user 1, the error values are minimum at all frequencies as it maintains four independent data streams and the errors are further reduced at 140 GHz as compared to 28 GHz and 73 GHz frequencies. Users who maintain three or two data streams have minimum errors in data transmissions at 143 GHz compared to 28 GHz and 73 GHz. This justifies the use of THz frequencies and higher order modulation schemes to achieve higher bandwidths, data rates, and spectral efficiencies. User 2 that maintains only one data stream has the highest errors in transmission, however the alternate users who have same number of independent data streams lead to lower error values. The common observation is that alternate users with same number of data streams suffer from higher transmission errors. From the overall results of the proposed system at 140 GHz frequency bands comparing with mmWave frequencies of 28 GHz and 73 GHz, strongly recommends to explore and use the frequencies beyond 100 GHz for next-generation wireless systems.

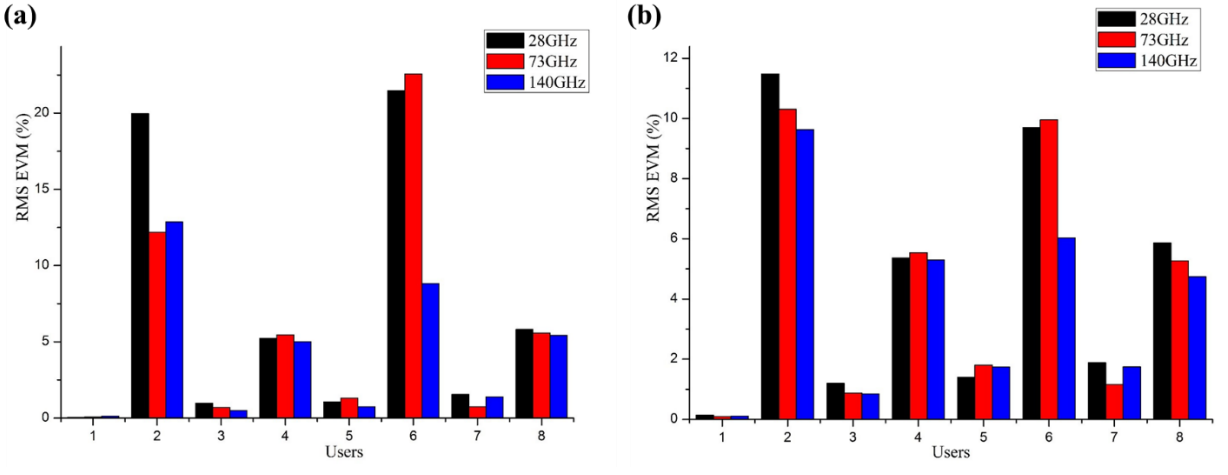

Fig. 7 Values of RMS error vectors in a MU-mMIMO hybrid beamforming system using 256-QAM modulation scheme with different number of BS antennas.

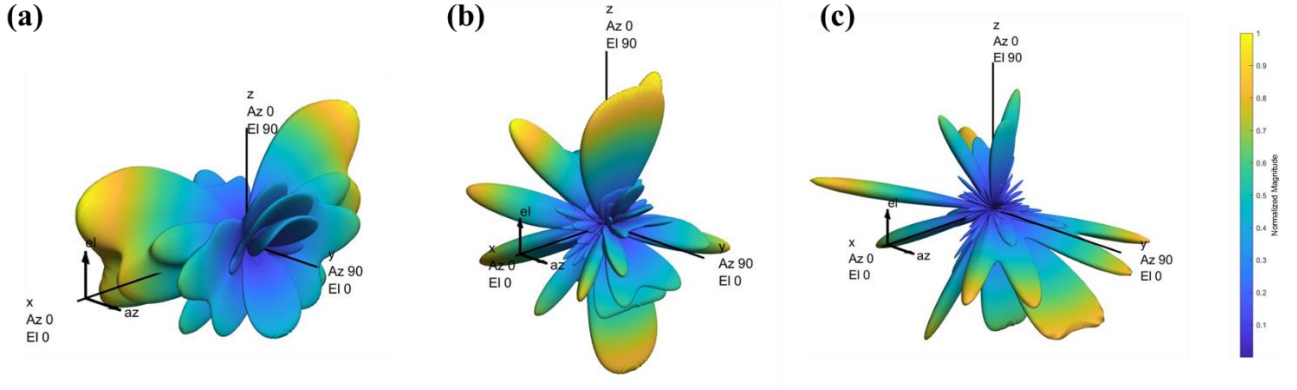

Fig. 8 3D-Radiation pattern of MU-mMIMO hybrid beamforming system using 256-QAM with different BS antennas for 8 users at 140 GHz.

© Engineered Science Publisher LLC 2021

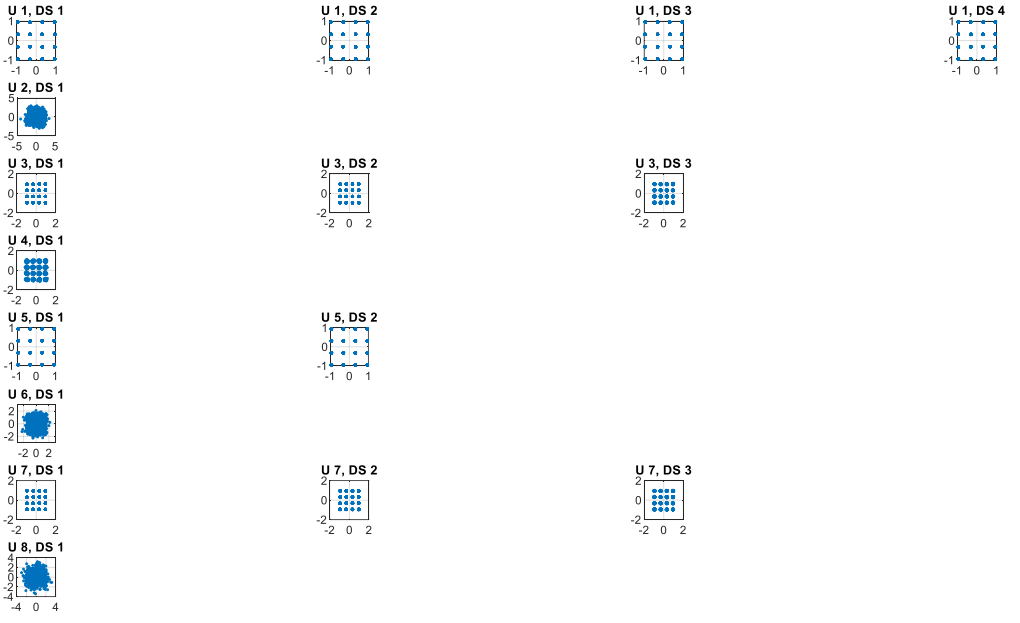

Fig. 9 Representation of symbol constellation (or data streams) using 16-QAM modulation with 64 BS antennas for 8 users at 140GHz.

Figs. 9, 10a and 10b indicate the equalized symbol constellation/data stream with various combinations of antennas array sizes and QAM schemes for an eight user mMIMO hybrid beamforming system. From the received symbol constellations of all combinations shown, it is evident that the variance of recovered data streams at Rx is minimum for users with more independent data streams as symbol points are present with less dispersion in the symbol constellation. The fact is that the data streams using the most dominant mode of MIMO scattering channel have maximum SNR values, but users with one independent data stream only have highly dispersed received symbols and it is very difficult to estimate the actual transmitted symbols.

This higher variance in the received symbols is due to fact that the lack of dominant modes in channel leads to poor SNR. However, the dispersion is very much reduced with increasing size of antenna arrays at BS and UE as shown in Figs. 9, 10a and 10b. Therefore, it is essential to use higher order antenna arrays to achieve higher spectral efficiency.

6. Conclusions and future scope

In this paper, a MU-ultra-mMIMO system is designed for THz frequencies with many independent data streams/user. Rigorous analysis is performed with different QAM modulation orders as well as antenna array configurations at Tx and Rx. The results of MU-ultra-mMIMO hybrid beamforming system at THz and mmWave frequencies are compared to prove the feasibility of using THz frequencies for next-generation wireless communication systems. For a 4-user mMIMO hybrid beamforming systems, it is suggested to use 256 × 8, 128 × 16, and 64 × 16 mMIMO system configurations where number of independent data streams/user are 2, 4, and 8, respectively. At the same time, for 8-user mMIMO hybrid beamforming systems, it is suggested to use 256 × 16 mMIMO

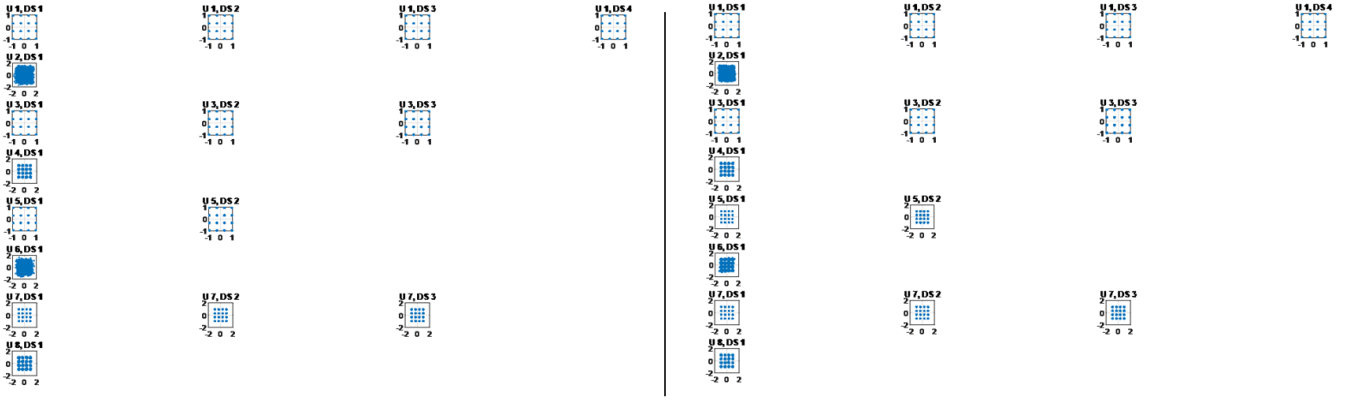

(a) 128 BS Antennas (a) 256 BS Antennas

Fig. 10 Representation of symbol constellation (or data streams) using 16-QAM modulation with 128 and 256 BS antennas for 8 users at 140 GHz.

© Engineered Science Publisher LLC 2021

antenna array configurations where users maintain four independent data streams/user. In both 4-user mMIMO and 8-user mMIMO hybrid beamforming, if the user has only one independent data stream then it is essential to have higher order mMIMO antenna arrays at BS and UE in which case a 256 × 4 mMIMO configuration is suitable. From the overall results of research work carried out at 140 GHz, main observation is that for users with minimum number of data streams, error values in their data streams are higher, whereas for users with maximum data streams, error values in their data streams are minimum. Therefore, it is strongly suggested to maintain multiple number of independent data streams/user to minimize the RMS EVM values and achieve higher order throughputs. However, hybrid beamforming designs for MU-mMIMO systems with an objective of minimizing errors and achieve higher throughput for users with minimum number of data streams needs to be carried out as a future research direction. Future work also includes performance analysis of the proposed MU-mMIMO hybrid beamforming system for ultra-mMIMO antenna array configurations of order 1024 × 1024 at 0.2, 0.34 and 0.4 THz frequency bands as the atmospheric absorption loss beyond Frii's free space path loss of the signal is minimum.

Conflict of interest

There are no conflicts to declare.

Supporting information

Not applicable.

Glossary

3D	three dimensional
3GPP	3rd generation partnership project
5G	fifth generation
6G	sixth generation
AI	artificial intelligence
AWGN	additive white gaussian noise
BCI	brain computer interactions
BS	base station
CRAS	connected robotics and autonomous systems
CSIT	CSI at Tx
D2D	device-to-device
DLT	distributed ledger technologies
EM	electromagnetic
eMBB	enhanced mobile broadband
EVM	error vector magnitude
FBMC	filter bank multi carrier
GFDM	generalized frequency division multiplexing
IIoT	industrial IoT
IoE	internet of everything
IoS	internet of space
IoT	internet of things
LDPC	low density parity check
LOS	line of sight
MBRLLC	mobile broadband reliable low latency communication
MIMO	multi-input-multi-output
mMIMO	massive MIMO
mMTC	massive machine type communication
mmWave	millimeter wave
MS	mobile station
MU	multi user
mURLLC	massive URLLC
NLOS	non-line of sight
NOMA	non-orthogonal multiple access
OAM	orbital angular momentum
OFDM	orthogonal frequency division multiplexing
OMA	orthogonal multiple access
QAM	quadrature amplitude modulation
RF	radio frequency
RIS	reconfigurable intelligent surfaces
RMS	root mean square
Rx	receiver
SNR	signal-to-noise ratio
SVD	singular value decomposition
THz	terahertz
T-R	transmit-receive
Tx	transmitter
UAV	unmanned aerial vehicle
UE	user equipment
ULA	uniform linear array
URA	uniform rectangular array
URLLC	ultra reliability and low latency communication
VLC	visible light communication
XR	extended reality

References

[1] M.H. Alsharif, A.H. Kelechi, M.A. Albreem, S.A. Chaudhry, M.S. Zia, S. Kim, *Symmetry*, 2020, **12**, 1-21, doi: 10.3390/sym12040676.

[2] G. Gui, M. Liu, F. Tang, N. Kato, F. Adachi, *IEEE Wirel. Commun.*, 2020, **27**, 126–132, doi: 10.1109/mwc.001.1900516.

[3] F. Qamar, M.U.A. Siddiqui, M.N. Hindia, R. Hassan, Q.N. Nguyen, *Electronics*, 2020, **9**, 1-39, doi: 10.3390/electronics9091416.

[4] P. Yang, Y. Xiao, M. Xiao, S. Li, *IEEE Network*, 2019, **33**, 70-75, doi: 10.1109/MNET.2019.1800418.

[5] R. Dilli, 2nd International Conference on Innovative Mechanisms for Industry Applications (ICIMIA), Bangalore, India, 2020, 767–772, doi:10.1109/ICIMIA48430.2020.9074973.

[6] V. Petrov, J.M. Eckhardt, D. Moltchanov, Y. Koucheryavy, T. Kurner, 14th European Conference on Antennas and Propagation (EuCAP), Copenhagen, Denmark, 2020, 1–5, doi: 10.23919/EuCAP48036.2020.9135389.

[7] G.R. MacCartney, S. Deng, S. Sun, T.S. Rappaport, IEEE 84th Vehicular Technology Conference (VTC-Fall), Montreal, QC, Canada, 2017, 1–6, doi: 10.1109/VTCFall.2016.7881087.

© Engineered Science Publisher LLC 2021

[8] S. Ju, S.H.A. Shah, M.A. Javed, J. Li, G. Palteru, J. Robin, Y. Xing, O. Kanhere, T.S. Rappaport, 2019 IEEE International Conference on Communications (ICC), Shanghai, China, 2019, 1–7, doi: 10.1109/ICC.2019.8761205.
[9] A.A. Goulianos, A.L. Freire, T. Barratt, E. Mellios, P. Cain, M. Rumney, A. Nix, M. Beach, 2017 IEEE 86th Vehicular Technology Conference (VTC-Fall), Toronto, ON, Canada, 2017, 1–5, doi: 10.1109/VTCFall.2017.8288373.
[10] L. Pometcu, R. D'Errico, 12th European Conference on Antennas and Propagation (EuCAP 2018), London, UK, 9–13 April 2018, 1–4, doi: 10.1049/cp.2018.0991.
[11] "Specific attenuation model for rain for use in prediction methods, propagation in non-ionized media," ITU-R. Tech. Rep. (P.838-3., 2005)
[12] J. Ma, J. Adelberg, R. Shrestha, L. Moeller, D.M. Mittleman, J. Infrared Millim. Terahertz Waves, 2018, **39**, 505–508, doi: 10.1007/s10762-018-0486-2.
[13] "Attenuation by Atmospheric Gases and related effects." ITU-R. Tech. Rep. (Recommendation ITU-R P.676-12, 2019).
[14] J.H. Zhang, P. Tang, L. Yu, T. Jiang, L. Tian, *Front. Inf. Technol. Electron. Eng.*, 2020, **21**, 39–61, doi: 10.1631/fitee.1900450.
[15] G.R. MacCartney, T.S. Rappaport, *IEEE J. Sel. Areas Commun.*, 2017, **35**, 1402–1418, doi: 10.1109/jsac.2017.2687838.
[16] S. Priebe, C. Jastrow, M. Jacob, T. Kleine-Ostmann, T. Schrader, T. Kurner, *IEEE T. Antenn. Propag.*, 2011, **59**, 1688–1698, doi: 10.1109/tap.2011.2122294.
[17] K. Guan, G. Li, T. Kurner, A.F. Molisch, B. Peng, R. He, B. Hui, J. Kim, Z. Zhong, *IEEE Trans. Veh. Technol.*, 2017, **66**, 5658–5674, doi: 10.1109/tvt.2016.2624504.
[18] K. Guan, B. Peng, D. He, J.M. Eckhardt, H. Yi, S. Rey, B. Ai, Z. Zhong, T. Kurner, *IEEE T. Antenn. Propag.*, 2021, **69**, 1007–1019, doi: 10.1109/tap.2020.3016399.
[19] S. Bhardwaj, N.K. Nahar, J.L. Volakis, *Microw. Opt. Technol. Lett.,* 2017, **59**, 415–423, doi: 10.1002/mop.30307.
[20] Y. Xing, T.S. Rappaport, 2018 IEEE Global Communications Conference (GLOBECOM), Abu Dhabi, United Arab Emirates, 2018, 1–6, doi: 10.1109/GLOCOM.2018.8647921.
[21] S. Kim, W.T. Khan, A. Zajic, J. Papapolymerou, *IEEE T. Antenn. Propag.*, 2015, **63**, 3198–3207, doi: 10.1109/tap.2015.2426831.
[22] G.R. MacCartney, T.S. Rappaport, S. Sun, S. Deng, *IEEE Access*, 2015, **3**, 2388–2424, doi: 10.1109/access.2015.2486778.
[23] G.R. MacCartney, T.S. Rappaport, *IEEE J. Sel. Areas Commun.*, 2017, **35**, 1663–1677, doi: 10.1109/jsac.2017.2699359.
[24] Q. Xia, J.M. Jornet, *IEEE Trans. Veh. Technol.*, 2019, **68**, 7804–7814, doi: 10.1109/tvt.2019.2924820.
[25] I. F. Akyildiz, A. Kak, S. Nie, *IEEE Access*, 2020, **8**, 133995-134030, doi: 10.1109/ACCESS.2020.3010896.
[26] J. Ma, R. Shrestha, L. Moeller, D.M. Mittleman, *Apl. Photonics*, 2018, **3**, 051601, doi: 10.1063/1.5014037.
[27] J. Kokkoniemi, J. Lehtomäki, M. Juntti, 10th European Conference on Antennas and Propagation (EuCAP), Davos, Switzerland, 2016, 1–5, doi: 10.1109/EuCAP.2016.7481176.
[28] R. Chataut, R. Akl, *Sensors*, 2020, **20**, 1-35, doi: 10.3390/s20102753.
[29] M. Giordani, M. Polese, A. Roy, D. Castor, M. Zorzi, *IEEE Commun. Surv. Tutor.*, 2019, **21**, 173–196, doi: 10.1109/comst.2018.2869411.
[30] R. Dilli, *Wireless Netw*, 2021, **27**, 1925–1939, doi: 10.1007/s11276-021-02546-w.
[31] S. Sun, T.S Rappaport, R.W. Heath, A.R. Nix, S. Rangan, *IEEE Commun. Mag.*, 2014, **52**, 110–121, doi: 10.1109/mcom.2014.6979962.

Author information

Ravilla Dilli *is currently working as Assistant Professor (Selection Grade) in Department of Electronics and Communication Engineering at Manipal Institute of Technology, Manipal Academy of Higher Education, Manipal, Karnataka, India. He has completed his Bachelor of Technology from Jawaharlal Nehru Technological University (JNTUH), Hyderabad, India and Master of Engineering in Applied Electronics from Satyabhama University, Chennai, India. He has completed his Ph.D. in the year 2018 from JNTUH, Hyderabad, India. He holds 4 best research paper awards to his credit and has published 32 research papers in National, International Journals and Conference Proceedings. He has 18 years of teaching and research experience in the fields of Internet of Things, 5G and 6G Wireless Technologies, Communication Networks, Network Security, Mobile Communication Systems, Routing Protocols in Mobile Ad hoc Networks (MANETs) and Wireless Sensor Networks, Vehicular Ad hoc Networks (VANETs). As a technical program committee member, he has reviewed more than 120 research articles for Scopus/Web of Science Journals include IEEE Transactions on Communications, IEEE Access, International Journal of Electronics, Journal of Experimental & Theoretical Artificial Intelligence, International Journal of Wireless Information Networks, Indonesian Journal of Electrical Engineering and Computer Science, International Journal of Informatics and Communication Technology (IJ-ICT), International Journal of Electrical and Computer Engineering,*

© Engineered Science Publisher LLC 2021

International Journal of Computer Engineering Research, also International Conferences sponsored by IEEE and Springer.

Ravi Chandra M L *is currently working as Professor and Head in Department of Electronics and Communication Engineering at Srinivasa Ramanujan Institute of Technology, Ananthapuramu, Andhra Pradesh, India. He has completed his Bachelor's degree and Master's degree from Jawaharlal Nehru Technological University (JNTUH), Hyderabad. He has completed his Ph.D. in the year 2015 from JNTUH, Hyderabad, India. He has published 20 research papers in National and International Journals and Conference Proceedings. He has 20 years of teaching and research experience in the fields of Digital Communications, Network Security, Routing Protocols in Wireless Sensor Networks, Vehicular Ad hoc Networks (VANETs). As a technical program committee member, he has reviewed more than 60 research articles for Scopus/Web of Science Journals.*

Deepthi Jordhana *obtained her B.Tech degree in Electronics and Communication Engineering and Master of Technology in Digital Systems and Computer Electronics, from RGMCET, Affiliated to JNTUH, Andhra Pradesh, India. She obtained his Ph.D. from JNTUA, University, Ananthapuramu, Andhra Pradesh, India. She has worked at various engineering colleges in Andhra Pradesh as Assistant Professor, Associate Professor, Professor and Head of the Department. Presently she is working as a Professor for ECE Department at Srinivasa Ramanujan Institute of Technology, Ananthapuramu, Andhra Pradesh, India from November, 2016 till date. She is having 17 years of teaching experience. She has 15 technical publications in International Journals and International Conferences. He is a life member of IE(I) and ISTE. Her Research areas are Wireless Communications, Digital Image Processing and Machine Learning.*

Publisher's Note: Engineered Science Publisher remains neutral with regard to jurisdictional claims in published maps and institutional affiliations.

 © Engineered Science Publisher LLC 2021